ISIJ International, Vol. 33 (1993), No. 7, pp. 775–782

Effects of Second Phase Morphology on Retained Austenite Morphology and Tensile Properties in a TRIP-aided Dual-phase Steel Sheet

Koh-ichi SUGIMOTO, Masahiro MISU,[1] Mitsuyuki KOBAYASHI[2] and Hidenori SHIRASAWA[3]

Department of Functional Machinery and Mechanics, Shinshu University, Tokida, Ueda, Nagano-ken, 386 Japan. 1) Formerly Graduate School, Shinshu University. Now at Car Body Design Department, Toyota Motor Corp., Toyota, Toyota, Aichi-ken, 471 Japan. 2) Department of Mechanical Systems Engineering, Shinshu University, Wakasato, Nagano, Nagano-ken, 380 Japan. 3) Kakogawa Works, Kobe Steel, Ltd., Kanazawa-cho, Kakogawa, Hyogo-ken, 675-01 Japan.

(Received on December 22, 1992; accepted in final form on April 15, 1993)

The relationship between second phase morphology and retained austenite morphology and the influences of these two kinds of morphology on tensile properties of a 0.17C–1.41Si–2.00Mn (mass%) TRIP-aided dual-phase steel have been investigated in a temperature range between 20 and 400°C.

A large amount of fine retained austenite was obtained when the second phase morphology was "a network structure" or "an isolated fine and acicular one." The retained austenite particles were nearly isolated in the ferrite matrix away from bainite islands and were moderately stable. On the other hand, "an isolated coarse structure" of second phase resulted in a small amount of more stable retained austenite film along bainite lath boundary.

The influence of second phase morphology on the flow curve significantly differed from that of a conventional ferrite–martensite dual-phase steel. Isolated retained austenite particles lowered the flow stress, and resultantly reduced the effects of second phase morphology (*i.e.*, network effect or fine grain size effect) on flow stress. However, the isolated retained austenite particles enhanced effectively the ductility, particularly at 50–100°C, due to the moderate strain induced transformation. On the other hand, retained austenite films along bainite lath boundary scarcely influenced on tensile properties of the steel. These results were discussed on the basis of a continuum theory.

KEY WORDS: transformation induced plasticity; dual-phase steel, high strength steel; morphology; retained austenite; second phase, ductility; tensile property; network structure; continuum theory.

1. Introduction

In general, retained austenite particles in a dual-phase steel transform to martensite during straining at room temperature.[1–3] Such strain-induced transformation will enhance ductility of the steel if the retained austenite particles are moderately stable against straining. In a conventional ferrite–martensite ($\alpha+\alpha'$) dual-phase steel, however, the retained austenite particles are so small in quantity and so unstable that the effect on ductility seems to be slight.[1–3] Recently, a new type of 600–1 000 MPa grade high-strength ferrite–(bainite plus retained austenite) dual-phase steel[4–9] containing a significant amount of stable retained austenite *i.e.*, "a TRIP-aided dual-phase steel", was developed by means of austempering immediately after intercritical annealing and further silicon addition of about 1.5 mass%. Excellent ductility of the steel due to transformation induced plasticity (TRIP)[10] of retained austenite will be expected to realize stretch-forming and deep-drawing of automotive parts, which have been impossible up to the present.

Ductility of TRIP-aided dual-phase steels is mainly controlled by M_s temperature[8] and volume fraction[8,9] of retained austenite. Therefore, further improvement of ductility is supposed to be attained by suppressing moderately the strain induced transformation, namely, (1) stabilizing the retained austenite and increasing the initial volume fraction by adding carbon, manganese, silicon, aluminum and so on[4–8], and (2) using warm forming.[6,8,9] Optimizing morphology of the second phase (bainite plus retained austenite) may be expected to enhance the ductility by suppressing void formation and plastic relaxation of internal stress,[11] or by changing retained austenite morphology, volume fraction and stability. However, there is apparently few studies[12] from such a point of view up to date.

In the present article, we investigated using a 0.17C–1.41Si–2.00Mn (mass%) TRIP-aided dual-phase steel (1) the effects of the second phase morphology on retained austenite morphology, volume fraction and stability, and (2) the effects of these two kinds of morphology on tensile properties at temperatures between 20 and 400°C. These results were discussed using a continuum theory.[11,13,14]

2. Experimental Procedure

A vacuum melted and cold-rolled steel sheet of 1.2 mm thickness supplied by Kobe Steel, Ltd. was used in the present study. The chemical composition, in mass%, was 0.17 C, 1.41 Si, 2.00 Mn, 0.014 P, 0.001 S, and 0.0042 N. After machining JIS-13B type tensile specimens of 50 mm gauge length by 12.5 mm width parallel to the rolling direction, the specimens were heat-treated in salt baths to obtain three types of second phase morphology, *i.e.*, TYPE I–III, with equal second phase volume fraction of about 0.4, as shown in **Fig. 1**. The structure after first stage of the heat-treatment was ferrite–pearlite for TYPE I and TYPE II, and martensite for TYPE III. The following intercritical annealing at $T_1 = 730°C$ (TYPE II) or 770°C (TYPE I, TYPE III) followed by austempering at 400°C for 1 000 sec were performed to obtain dual-phase structure containing a significant amount of retained austenite. Hereafter, each steel heat-treated as illustrated in Fig. 1 is called TYPE I, TYPE II or TYPE III steel, respectively. According to the work[12] of the authors, maximum total elongation for each steel is obtained when the second phase volume fraction is about 0.4.

Line intersecting method was used to obtain volume fraction of the second phase. The amount of retained austenite was quantified by X-ray diffractometry using Mo-$K\alpha$ radiation. To minimize the effect of texture, the volume fraction of retained austenite was calculated on the basis of integrated intensity of 200_α, 211_α, 200_γ, 220_γ, and 311_γ diffraction peaks.[15] Carbon concentration of retained austenite C_γ (mass%) was estimated from the lattice parameter a_γ ($\times 10^{-10}$ m) measured from 220_γ diffraction peak of Cr-$K\alpha$ radiation using Eq. (1).[16]

$$a_\gamma = 3.5467 + 0.0467 C_\gamma \quad \text{.....(1)}$$

Tensile testing was carried out on a hard type tensile testing machine at temperatures from 20 to 400°C and at a strain rate of 2.8×10^{-4}/s. The samples were directly heated using a pair of strip-heaters (70 mm × 90 mm) during tension testing.

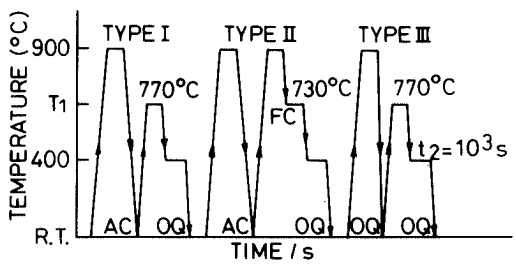

Fig. 1. Heat treatment diagrams. Holding time at 900°C and T_1 is 1 000 sec. "FC", "AC" and "OQ" in the figure represent furnace cooling, air cooling and quenching in oil, respectively.

3. Results

3.1. Morphology and Properties of Retained Austenite

Figure 2 shows scanning electron micrographs of the as-austempered samples. Volume fraction of second phase f and initial volume fraction $f_{\gamma 0}$ and carbon concentration C_γ of retained austenite in the steels are shown in **Table 1**. From Fig. 2 and Table 1, the second phase of each steel is found to be composed of bainite and retained austenite, as reported already by other

Table 1. Metallurgical parameters of each steel.

TYPE	f	$f_{\gamma 0}$	a_γ ($\times 10^{-10}$ m)	C_γ (mass%)	$f_{\gamma 0} \times C_\gamma$ (mass%)
I	0.43	0.119	3.6002	1.15	0.137
II	0.41	0.066	3.6092	1.34	0.088
III	0.40	0.131	3.6054	1.26	0.165

f: Volume fraction of second phase.
$f_{\gamma 0}$, a_γ, C_γ: Initial volume fraction, lattice parameter and carbon concentration of retained austenite, respectively.

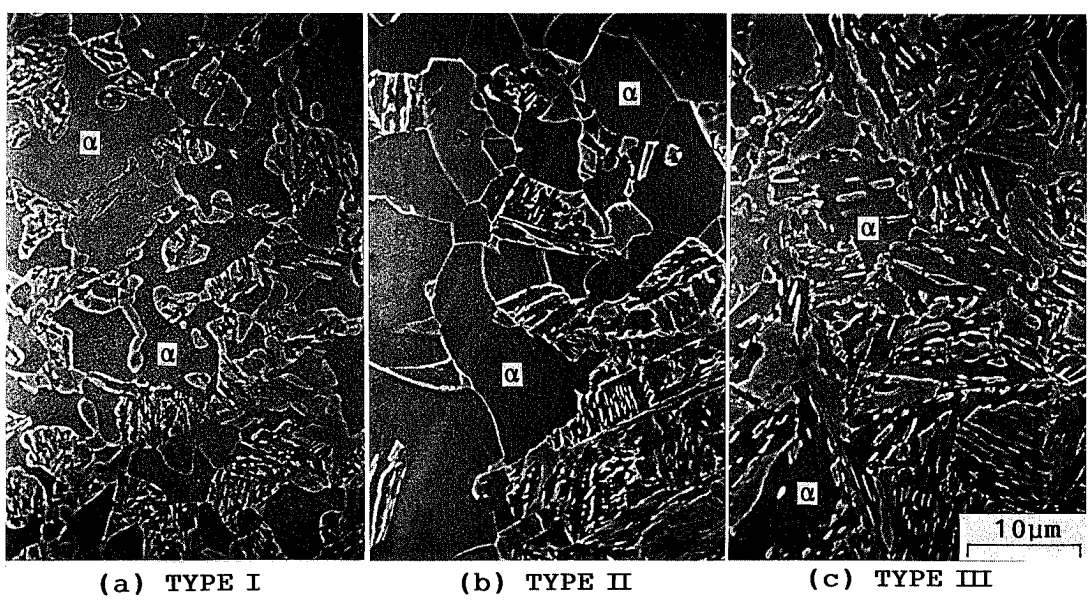

Fig. 2. Scanning electron micrographs of (a) TYPE I, (b) TYPE II and (c) TYPE III steels, which are intercritically annealed at 770°C (TYPE I, TYPE III) or 730°C (TYPE II), followed by immersing in salt bath held at 400°C for 1 000 sec. A letter "α" in the photograph represents ferrite matrix.

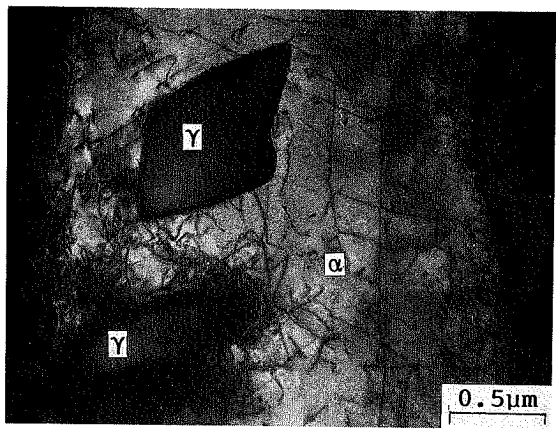

(a) TYPE I

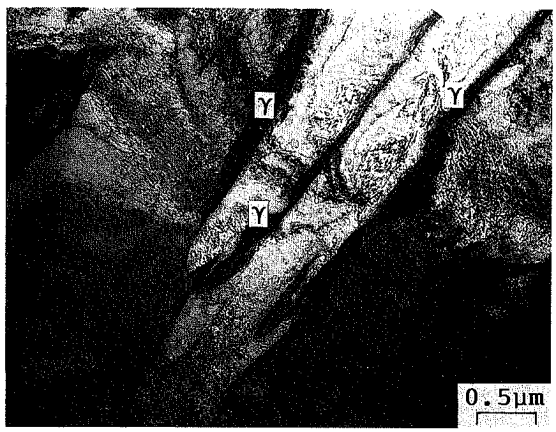

(b) TYPE II

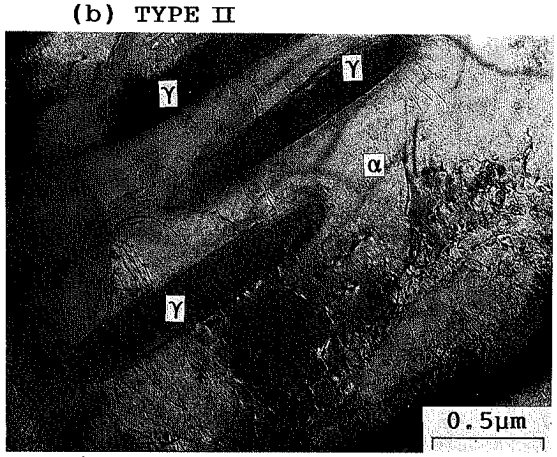

(c) TYPE III

Fig. 3. Transmission electron micrographs showing (a) isolated retained austenite (γ) islands in ferrite (α) matrix in TYPE I steel, (b) retained austenite films along bainite lath boundary in TYPE II steel, and (c) isolated acicular retained austenite particles in ferrite matrix in TYPE III steel.

workers.[4-9] The second phase morphology of TYPE I, TYPE II and TYPE III steels can be classified as (a) a network structure along the ferrite grain boundary, (b) an isolated coarse one, and (c) an isolated fine and acicular one, respectively. The network structure, however, is somewhat imperfect compared to that of an $\alpha+\alpha'$ dual-phase steel,[11] as shown in Fig. 2(a). The morphology of each steel is resemble to austenite morphology on intercritical annealing.

Figure 3 shows transmission electron micrographs of retained austenite morphology of the as-austempered steels. In TYPE I steel, it is found that retained austenite particles less than 1 μm are isolated in the ferrite matrix or on the grain boundary, away from or adjacent to the bainite particles, as shown in Fig. 3(a). A few dislocations and/or stacking faults are observed in some retained austenite islands. In TYPE III steel, similar isolated retained austenite islands also appear on the previous martensite lath boundary obtained by first stage of heat-treatment (Fig. 1) although they are fine and acicular, as shown in Fig. 3(c). For TYPE II steel, retained austenite films less than 0.1–0.2 μm width are confirmed to mainly exist along the bainite lath boundary, as shown in Fig. 3(b). Retained austenite morphology of these steels is summarized in **Table 2**.

Table 2. Morphology of second phase and retained austenite of each steel.

TYPE	Morphology	
	Second phase	Retained austenite
I	Network	Isolated island in ferrite matrix
II	Isolated	Thin film along bainite lath boundary
III	Isolated (fine and acicular)	Isolated fine and acicular island in ferrite matrix

A significant amount of retained austenite is obtained in TYPE I ($f_{\gamma 0}=0.119$) and TYPE III steels ($f_{\gamma 0}=0.131$), whose carbon concentrations in retained austenite (1.15, 1.26 mass%, respectively) are lower than that in TYPE II steel (1.34 mass%), as shown in Table 1. The total carbon concentration ($C_\gamma \times f_{\gamma 0}$), however, is higher in TYPE I and TYPE III steels. This indicates that a large amount of carbon-enriched retained austenite particle is obtained when austenite phase on intercritically annealing distributes along ferrite grain boundary or subgrain boundary, but not when the austenite is blocky and coarse in the ferrite matrix.

3.2. Tensile Properties

Flow curves at various testing temperatures and testing temperature dependence of tensile properties for each TYPE steel are shown in **Figs. 4** and **5**, respectively. The influences of second phase morphology on the tensile properties are as follows.

3.2.1. Tensile Properties at 20°C

Continuous yielding appears on flow curves for all TYPE steels. Only in TYPE III steel, however, it is followed by yield plateau due to a substructure.[11,12] Flow stress and strain hardening rate in a small strain range below 5% and total elongation are particularly influenced by second phase morphology. Higher flow stress and strain hardening rate in the small strain range appears in TYPE II steel, although a difference in flow stress between the steels is slight. This result differs from that obtained in an $\alpha+\alpha'$ dual-phase steel (0.11C–0.22Si–1.36Mn steel, in mass%)[11] as shown in **Fig. 6**. In Fig. 6, flow stress and strain hardening rate of TYPE II steel is the lowest of all TYPE steels because

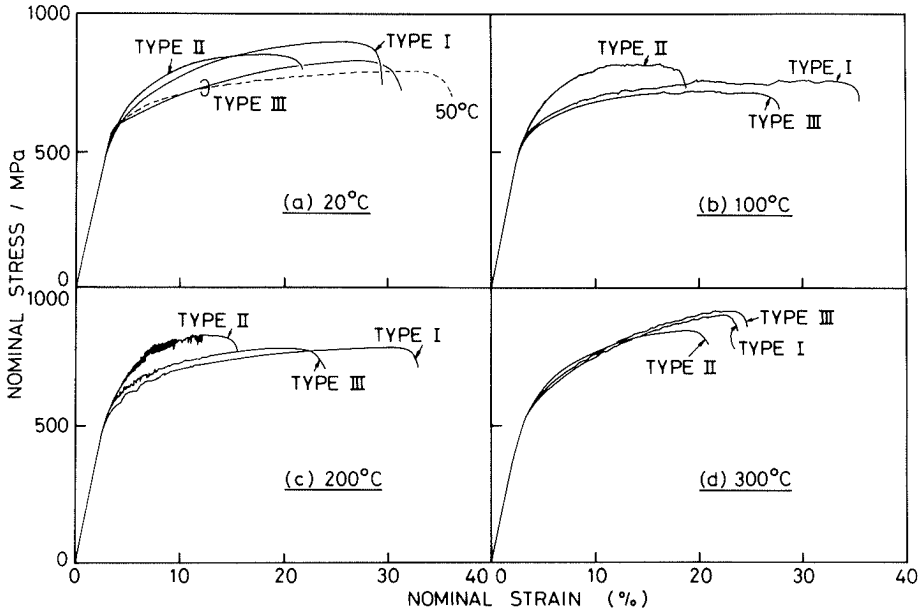

Fig. 4.
Nominal stress–strain curves at various testing temperatures of each steel with $f \fallingdotseq 0.4$.

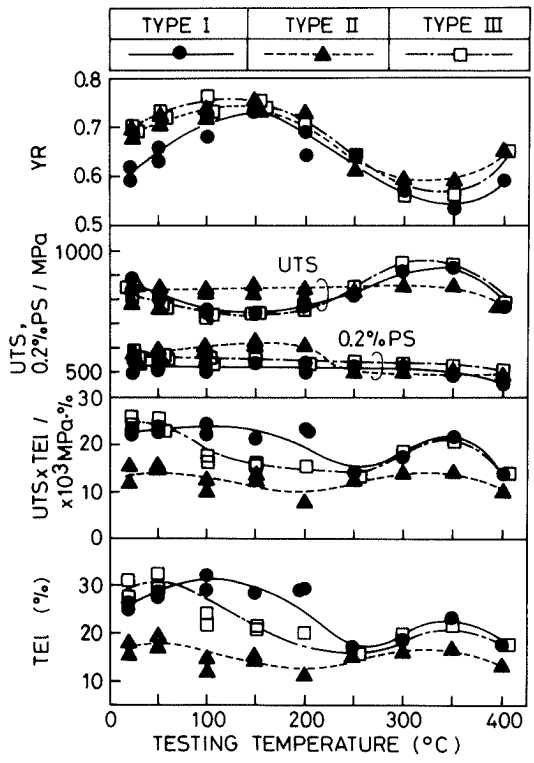

0.2% PS: 0.2% proof stress, UTS: Ultimate tensile strength, YR: Yield ratio (=0.2% PS/UTS), TEl: Total elongation, UTS × TEl: Strength–ductility balance.

Fig. 5. Testing temperature dependence of tensile properties of each steel.

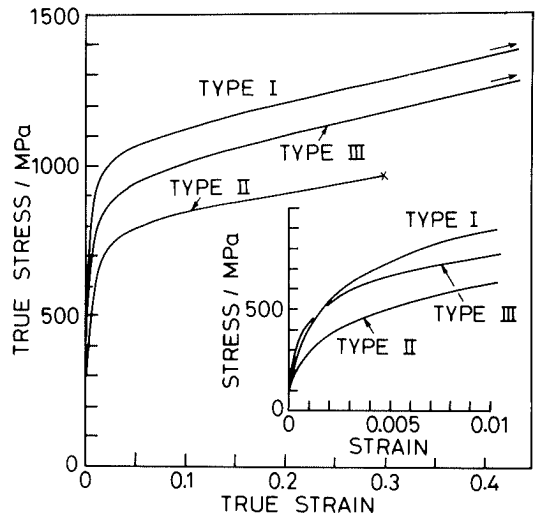

Fig. 6. True stress–true strain curves of each TYPE of an $\alpha+\alpha'$ dual-phase steel (0.11C–0.22Si–1.36Mn steel)[11] with $f \fallingdotseq 0.5$.

of coarse grain size and larger plastic relaxation of internal stress. The effect of network structure observed in TYPE I of the $\alpha+\alpha'$ dual-phase steel, namely constraining deformation of ferrite and resultantly occurring large strain hardening in a small strain range, also appears in the present TYPE I steel, but it is smaller than that of the $\alpha+\alpha'$ dual-phase steel.

Large total elongation (TEl) and strength–ductility balance (UTS × TEl) are obtained in TYPE III steel. They are inferior only a little in TYPE I steel, but are conspicuously small in TYPE II steel. This tendency agrees well with that of the $\alpha+\alpha'$ dual-phase steel. From Fig. 4(a), good ductility of TYPE I and TYPE III steels is found to be caused by moderate strain hardening in a large strain range prior to onset of necking. The strain hardening mechanism, however, differs from each other as mentioned in the Sec. 4.2.

3.2.2. Testing Temperature Dependence of Tensile Properties

Remarkable testing temperature dependence of tensile properties, particularly total elongation and ultimate tensile strength (UTS), appears in a temperature range from 20 to 200°C for TYPE I and TYPE III steels, but not for TYPE II steel. The ultimate tensile strength becomes minimum at about 150°C for both TYPE I and TYPE III steels with severe serrations and lower strain hardening in a small strain range. The total elongation and strength–ductility balance show a peak at 100°C (TYPE I) or 50°C (TYPE II and TYPE III). At

the peak temperature, the maximum values of TYPE I steel (TEl = 32%, TS × TEl = 24 000 MPa%) are nearly equal to those of TYPE III steel. And, in TYPE I and TYPE III steels, moderate strain hardening is maintained over larger strain range compared to that at 20°C, and resultantly onset of necking is retarded.

Serrations also appear on flow curve in a 0.006C–1.5Si–1.5Mn (mass%) ferritic steel[6] at temperatures higher than 100°C. Therefore, the serrations occurring in the present steel may be owing to dynamic strain-aging of the ferrite matrix as well as strain-induced transformation of the retained austenite[8]. At 300°C, a difference in flow stress between the steels is considerably small. The reason is under investigation.

3.3. Strain Induced Transformation Behavior of Retained Austenite

Generally, retained austenite particles in a TRIP-aided dual-phase steel transform gradually to α′-martensite with increasing strain below 200°C. The relationship between retained austenite content f_γ and tensile strain ε is given by the following Eq. (2).[9]

$$\log f_\gamma = \log f_{\gamma 0} - k \cdot \varepsilon \quad \text{.....(2)}$$

where k is a constant varying with testing temperature, and the lower the k-value the less the strain induced transformation takes place.

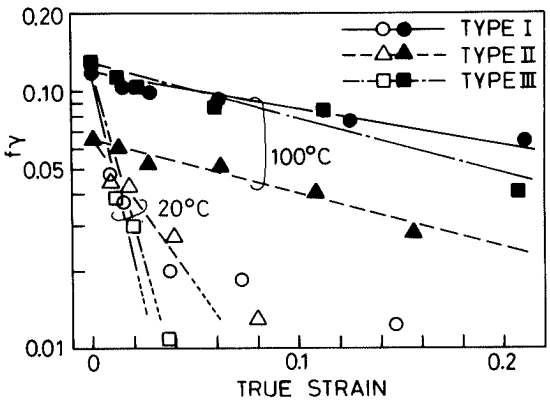

Fig. 7. Variations in retained austenite content f_γ during tensile straining at 20 and 100°C for each steel.

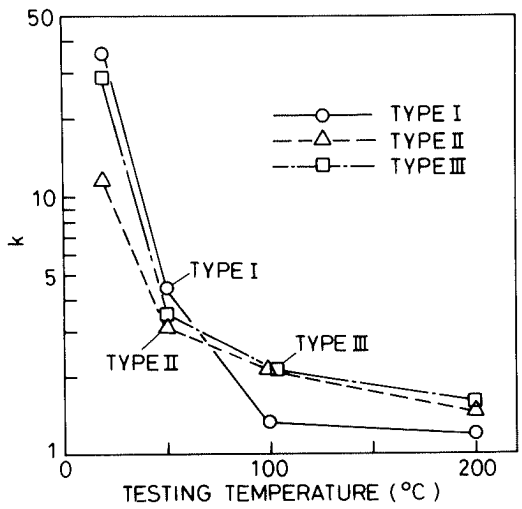

Fig. 8. Variations in k-value with testing temperature for each steel.

Figure 7 shows the variation in retained austenite content during tensile straining, and **Fig. 8** shows the k-values[9] obtained from a slope of straight line drawn in a range of $f_\gamma > 0.02$ in Fig. 7. At 20°C, the strain induced transformation of retained austenite in TYPE II steel is found to be considerably suppressed compared to those of TYPE I and TYPE III steels, although the transformation finishes within a small strain range less than about 0.05. With increasing the testing temperature, the strain induced transformation in all the steels is suppressed gradually, and the retained austenite becomes stable against straining above 100°C. A difference in retained austenite stability above 100°C between the steels can be ignored although the stability in TYPE I steel is lower than the other steels.

4. Discussion

4.1. Relation between Morphology and Stability of Retained Austenite

In general, retained austenite morphology in dual-phase steels is classified into two groups by the type of phase surrounding it as follows.

(1) Isolated retained austenite islands[1–3,5–9,17] lying in a soft ferrite matrix or on the grain boundary, adjacent to or away from the other hard second phases such as bainite[17] or martensite.

(2) Retained austenite thin films existing along martensite[18] or bainite lath boundary,[19] or blocky retained austenite in these hard second phases.[5]

The retained austenite morphology of both TYPE I and TYPE III of the present steel belongs to (1). On the other hand, the morphology in TYPE II steel belongs to (2) and most of the retained austenite lies as films along bainite lath boundary, as shown in Fig. 3(b). In such a case, M_s temperature of the retained austenite is expected to be mainly affected by hydrostatic pressure as well as carbon concentration.[8,9]

Generally, hydrostatic pressure constrains a volume expansion and shear deformation accompanied with strain induced martensite transformation. If an isotropic transformation strain expressed as $\varepsilon^* = 0.0058 + 0.0045 C_\gamma$ occurs on the martensite transformation, the resultant hydrostatic pressure σ_p can be estimated using the following Eq. (3) proposed by Sakaki *et al.*:[14]

$$\sigma_p = 2/3\{Y_0 + 2H_0\varepsilon^*\} + 2/3\, Y_0 \ln\{E\varepsilon^*/(1-\nu)Y_0\} \quad \text{.....(3)}$$

where Y_0, H_0 are yield stress and strain hardening rate of a given phase surrounding retained austenite particle, respectively. E and ν are respectively Young's modulus and Poisson's ratio, and are assumed to be equal for all the constituents.

From Eq. (3), high hydrostatic pressure of about 1 560 MPa occurs in retained austenite films of TYPE II steel, if $Y_0 = 1\,000$ MPa and $H_0 = 5\,000$ MPa for bainite phase,[20] $C_\gamma = 1.34$ mass%, $E = 206\,000$ MPa and $\nu = 0.28$. On the other hand, lower hydrostatic pressure of about 900 MPa arises in the ratained austenite islands of TYPE I and TYPE III steels, if $Y_0 = 400$ MPa and $H_0 = 1\,000$ MPa for ferrite phase[6] and $C_\gamma = 1.15$ (TYPE I) or

1.26 mass% (TYPE III). According to the work[21] of Radcliffe and Schatz using plain 0.3–1.2 mass% C steels, the M_s temperature decreases by about 6°C per hydrostatic pressure of 100 MPa. Therefore, M_s temperature of retained austenite in TYPE II steel should be estimated to be reduced by 40°C due to hydrostatic pressure, compared to other steels.

The relation between M_s temperature (°C) and concentration of carbon C_γ (mass%) and manganese Mn_γ (mass%) is shown by the following Eq. (4).

$$M_s = 550 - 360 \times C_\gamma - 40 \times Mn_\gamma \quad \text{.....(4)}$$

If the manganese concentration is assumed to be 1.5 times the added content on the basis of useful work of Gilmour and Schatz[21] and Speich *et al.*,[22] the M_s temperatures of retained austenite are calculated from Eq. (4) to be 17°C, −52°C, and −23°C for TYPE I, TYPE II, and TYPE III steels, respectively. Considering the above-mentioned decrease in M_s temperature due to hydrostatic pressure, resultant M_s temperature of retained austenite in TYPE II steel should be estimated to be lower by about 110 and 70°C than those of TYPE I and TYPE III steels, respectively. For the M_s temperatures, the effect of grain size is neglected for a lack of data reported.

According to the work[8,9] of the authors, strain induced transformation to martensite of retained austenite in TRIP-aided dual-phase steels occurs in a temperature range between M_s and M_d (which can not be measured by appearance of strain-induced bainite transformation[9]), and is suppressed with increasing testing temperature. Furthermore, k-value of the steels at a given temperature decreases with decreasing the M_s temperature of retained austenite. Therefore, lower k-values at 20 and 50°C in the present TYPE II steel, as shown in Figs. 7 and 8, can be explained by lower M_s temperature arising from higher hydrostatic pressure and carbon concentration as mentioned above. Lower k-values at 100 to 200°C in TYPE I steel is incompatible with the above reports.[8,9] Although this reason is under investigation, a difference in the k-value between these steels is considered to be little worth consideration.

4.2. Effects of Second Phase Morphology and Retained Austenite Morphology on Deformation Behavior

Generally, flow stress and strain hardening rate of the conventional $\alpha+\alpha'$ dual-phase steel is controlled by internal stress arising from a difference in flow stress between the ferrite matrix and second phase. The internal stress increases with increasing the second phase strength, but it is plastically relaxed due to secondary slip proposed by Ashby[24] or sliding at matrix/second phase interface if a ratio of second phase strength to ferrite strength is more than 3[25] and the second phase is an isolated structure.[11] In a large strain range, void formation behavior at matrix/second phase interface affects the strain hardening behavior as well as the above internal stress.[11]

The present steel has a large amount of stable retained austenite. Therefore, it is expected that the effects of second phase morphology on the flow curve considerably differ from those of the $\alpha+\alpha'$ dual-phase steel. In this section, mean flow stress of the second phase is estimated using a continuum theory.[11,13] And from the calculated result and strain induced transformation behavior in the Sec. 3.3, the effects of second phase morphology on characteritic deformation behavior are discussed.

4.2.1. Mean Flow Stress of Second Phase

In the present dual-phase steel, the second phase is composed of two kinds of hard phase, *i.e.*, bainite and retained austenite. The retained austenite gradually transforms to harder martensite during straining. In addition, there is a possible of occurrence of the plastic relaxation of internal stress. Thus, the second phase is replaced by "the hypothetical second phase[26]" whose flow stress σ_H is calculated from Eq. (5).[11,13]

$$\sigma(\varepsilon) = \sigma_S(\varepsilon_S) + fKE(\varepsilon_S - \varepsilon_H)$$
$$(\varepsilon_S - \varepsilon_H) = (\sigma_H(\varepsilon_H) - \sigma_S(\varepsilon_S))/KE \quad \text{.....(5)}$$
$$K = (7-5\nu)/10(1-\nu^2)$$

where $\sigma(\varepsilon)$, $\sigma_S(\varepsilon_S)$ and $\sigma_H(\varepsilon_H)$, respectively, represent flow stresses (plastic strain) of the dual-phase steel, ferrite matrix and hypothetical second phase, and f is volume fraction of the second phase.

Using Eq. (5) and experimental flow stress and second phase volume fraction of each steel (Fig. 4 and Table 1), proof stress of hypothetical second phase at 1% offset strain (where the second phase plastically deforms as well as the ferrite matrix) is respectively estimated to be 875, 970 and 885 MPa at 20°C or 800, 960 and 820 MPa at 100°C in TYPE I, II and III steels, if $\sigma_S(0) = 400$ MPa and the linear hardening rate H_S in a small strain range is 1 000 MPa. Only in TYPE II steel the calculated 1% offset stress is found to be nearly as high as experimental one of bainite phase (>1 000 MPa)[20] and to be independent on testing temperature. Such a result indicates that the retained austenite films in TYPE II steel hardly lower the mean strength of second phase. In addition, it is supposed that the deformation of the retained austenite films is constrained by harder bainite surrounding them, although they transform during straining (Figs. 7 and 8).

On the other hand, isolated retained austenite particles in TYPE I and TYPE III steels lower the mean strength of second phase in the small strain range. From the above calculated result, the retained austenite is estimated to have 1% proof stress of 500–600 MPa, lower than that of bainite phase. For each steel, a difference in 1% proof stress of hypothetical second phase between 20 and 100°C may be owing to strain-induced martensite content.

4.2.2. Deformation in a Small Strain Range below 5%

In a small strain range below 5%, higher flow stress and strain hardening rate at 20 to 200°C appeared for TYPE II steel (Fig. 4). This is considered to be mainly caused by higher second phase strength, independent on the testing temperature, as mentioned in the Sec. 4.2.1. For the present steel, a ratio of second phase strength to ferrite one is less than 3.[25] Therefore, plastic relaxation of internal stress is expected to be small compared to the $\alpha+\alpha'$ dual-phase steel. The small plastic relaxation may also contribute to higher flow stress of TYPE II steel as

well as high second phase strength.

In TYPE I steel, the effect of network structure on strain hardening rate was small compared to the $\alpha+\alpha'$ dual-phase steel,[11] and it decreased further with increasing testing temperature up to 200°C, as shown in Figs. 4 and 6. Higher strain hardening rate and flow stress at 20°C may be caused by a great increase in strain-induced martensite content at an early stage and resultant formation of a more interconnected network structure. On the other hand, lower strain hardening rate and flow stress at 50 to 200°C may result from an imperfect and soft network structure due to more stable retained austenite.

In TYPE III steel, an isolated structure of the second phase and retained austenite seems to result in low strain hardening rate and flow stress at 20 to 200°C, through larger plastic relaxation compared to TYPE I steel and low second phase strength similar to TYPE I steel.

4.2.3. Deformation in a large Strain Range

In TYPE I and TYPE III steels, large total elongation was obtained due to moderate strain hardening in a large strain range prior to onset of necking (Fig. 4). For investigating this reason, uniformly deformed area of the samples broken at 20 to 200°C was observed by optical microscopy. Any void at the ferrite/second-phase interface was scarcely detected in all the samples of TYPE III and in those of TYPE I broken at 50 to 200°C. There are a small number of fine voids at the interface in the sample broken at 20°C for TYPE I steel, while a great number of large voids were formed in all the broken samples of TYPE II. At 20°C, most of retained austenite in TYPE I and TYPE III steels transforms within a small strain range. Therefore, the above result indicates that the void formation of TYPE III steel is mainly controlled by fine grain size effect similar to the $\alpha+\alpha'$ dual-phase steel.[11] With increasing the testing temperature, local stress relaxation at the interface due to strain induced transformation[8,9] may play more important part for suppressing the void formation. This may also suppress void formation of TYPE I steel strained at 50 to 200°C as well as TYPE III steel.

From the above result, large total elongation of TYPE I steel at 20°C (*i.e.*, moderate strain hardening rate in the large strain range) is concluded to be mainly ascribed to a more perfect and harder network structure. Larger total elongation at 100°C seems to be mainly caused by TRIP effect[8,9] without void formation due to gradual strain induced transformation of retained austenite in the large strain range. In TYPE III steel, fine grain size effect plays an important role on the large total elongation as well as the above TRIP effect.

According to the work[8] of the authors using 0.2C–(1.0–2.5)Si–(1.0–2.5)Mn (mass%) TRIP-aided dual-phase steels, a peak temperature for total elongation increases with increasing M_s temperature of the retained austenite. For TYPE I and TYPE III steels, the relationship between peak temperature and M_s temperature agrees qualitatively with the above result. More detailed research is required for the peak temperature.

5. Conclusions

The effects of second phase morphology on volume fraction, stability and morphology of retained austenite in a 0.17C–1.41Si–2.00Mn(mass%) TRIP-aided dual-phase steel was investigated. In addition, the influence of these two kinds of morphology on tensile properties at temperatures between 20 and 400°C were examined. The results are summarized as follows.

(1) When the second phase morphology was a network structure along the ferrite grain boundary or an isolated fine and acicular one along previous martensite lath boundary, a large amount of carbon-enriched isolated austenite particle retained in the ferrite matrix, adjacent to or away from bainite. On the other hand, a small amount of retained austenite thin film was observed along bainite lath boundary, when the second phase had an isolated coarse structure. M_s temperature of the retained austenite films was estimated to decrease by 70 to 110°C compared to isolated retained austenite particles due to higher carbon concentration and higher hydrostatic pressure.

(2) A steel with a network structure (TYPE I) or an isolated fine and acicular one (TYPE III) of second phase had lower flow stress and greater ductility compared to a steel (TYPE II) with an isolated coarse structure of second phase. The lower flow stress of TYPE I and TYPE III steels was ascribed to softer isolated retained austenite particles. And the excellent ductility was concluded to be caused by TRIP effect of the retained austenite as well as the network effect or the fine grain size effect of second phase morphology itself. On the other hand, retained austenite films in TYPE II steel hardly influenced deformation behavior.

(3) With increasing testing temperature up to 200°C, isolated retained austenite particles in TYPE I and TYPE III steels enhanced ductility considerably, particularly at 50–100°C, due to a moderate increase in the stability. However, they relatively reduced the effects of network structure (*i.e.*, increasing the strain hardening rate) or of isolated fine and acicular one of second phase (*i.e.*, suppressing void formation at matrix/second phase interface). As a result, the flow stress of these steels decreased.

REFERENCES

1) J. M. Rigsbee and P. J. Verderarend: Formable HSLA and Dual-phase Steels, ed. by R. A. Kot and J. W. Morris, AIME, New York, (1977), 56.
2) A. R. Marder: Formable HSLA and Dual-phase Steels, ed. by R. A. Kot and J. W. Morris, AIME, New York, (1977), 89.
3) T. Furukawa, H. Morikawa, H. Takechi and K. Koyama: Structure and Properties of Dual-phase Steel Sheets, ed. by R. A. Kot and J. W. Morris, AIME, New York, (1979), 281.
4) O. Matsumura, Y. Sakuma and H. Takechi: *Trans. Iron Steel Inst. Jpn.*, **27** (1987), 570.
5) H. C. Chen, H. Era and M. Shimizu: *Metall. Trans.*, **20A** (1989), 437.
6) K. Sugimoto, M. Kobayashi and S. Hashimoto: *J. Jpn. Inst. Met.*, **54** (1990), 657.
7) Y. Sakuma, O. Matsumura and H. Takechi: *Metall. Trans.*, **22A** (1991), 489.
8) K. Sugimoto, N. Usui, M. Kobayashi and S. Hashimoto: *ISIJ*

Int., **32** (1992), 1311.
9) K. Sugimoto, M. Kobayashi and S. Hashimoto: *Metall. Trans.*, **23A** (1992), 3085.
10) V. F. Zackay, E. R. Parker, D. Fahr and R. Bush: *Trans. Amer. Soc. Met.*, **60** (1967), 262.
11) K. Sugimoto, T. Sakaki, T. Fukuzato and O. Miyagawa: *Tetsu-to-Hagané*, **71** (1985), 994.
12) K. Sugimoto, M. Misu, M. Kobayashi and H. Shirasawa: *Tetsu-to-Hagané*, **76** (1990), 1356.
13) Y. Tomota, K. Kuroki, T. Mori and I. Tamura: *Mater. Sci. Eng.*, **24** (1976), 85.
14) T. Sakaki, K. Sugimoto and T. Fukuzato: *Acta Metall.*, **31** (1983), 1737.
15) H. Maruyama: *J. Jpn. Soc. Heat Treat.*, **17** (1977), 198.
16) Z. Nishiyama: Martensite Transformation, Maruzen, Tokyo, (1971), 13.
17) J. J. Yi, K. J. Yu, I. S. Kim and S. J. Kim: *Metall. Trans.*, **14A** (1983), 1497.
18) N. J. Kim and G. Thomas: *Metall. Trans.*, **12A** (1981), 483.
19) R. L. Houillier, G. Begin and A. Dube: *Metall. Trans.*, **2** (1971), 2645.
20) K. Sugimoto and T. Sakaki: unpublished data, (1985).
21) S. V. Radcliffe and M. Schatz: *Acta Metall.*, **10** (1962), 201.
22) J. B. Gilmour, G. R. Purdy and J. S. Kirkaldy: *Metall. Trans.*, **3** (1972), 1455.
23) G. R. Speich, V. A. Demarest and R. L. Miller: *Metall. Trans.*, **12A** (1981), 1419.
24) M. F. Ashby: *Philos. Mag.*, **14**, (1966), 1157.
25) Y. Tomota and I. Tamura: *Tetsu-to-Hagané*, **68** (1982), 1147.
26) K. Sugimoto, T. Sakaki, M. Kobayashi and S. Yasuki: *J. Jpn. Inst. Met.*, **54** (1990), 1344.